NASA/TM—2012–215995

Orion Pad Abort 1 Crew Module Mass Properties Test Approach and Results

Claudia Herrera and Adam Harding

Dryden Flight Research Center, Edwards, California

March 2012

NASA STI Program ... in Profile

Since its founding, NASA has been dedicated to the advancement of aeronautics and space science. The NASA scientific and technical information (STI) program plays a key part in helping NASA maintain this important role.

The NASA STI program operates under the auspices of the Agency Chief Information Officer. It collects, organizes, provides for archiving, and disseminates NASA's STI. The NASA STI program provides access to the NASA Aeronautics and Space Database and its public interface, the NASA Technical Report Server, thus providing one of the largest collections of aeronautical and space science STI in the world. Results are published in both non-NASA channels and by NASA in the NASA STI Report Series, which includes the following report types:

- TECHNICAL PUBLICATION. Reports of completed research or a major significant phase of research that present the results of NASA Programs and include extensive data or theoretical analysis. Includes compilations of significant scientific and technical data and information deemed to be of continuing reference value. NASA counterpart of peer-reviewed formal professional papers but has less stringent limitations on manuscript length and extent of graphic presentations.

- TECHNICAL MEMORANDUM. Scientific and technical findings that are preliminary or of specialized interest, e.g., quick release reports, working papers, and bibliographies that contain minimal annotation. Does not contain extensive analysis.

- CONTRACTOR REPORT. Scientific and technical findings by NASA-sponsored contractors and grantees.

- CONFERENCE PUBLICATION. Collected papers from scientific and technical conferences, symposia, seminars, or other meetings sponsored or co-sponsored by NASA.

- SPECIAL PUBLICATION. Scientific, technical, or historical information from NASA programs, projects, and missions, often concerned with subjects having substantial public interest.

- TECHNICAL TRANSLATION. English-language translations of foreign scientific and technical material pertinent to NASA's mission.

Specialized services also include organizing and publishing research results, distributing specialized research announcements and feeds, providing help desk and personal search support, and enabling data exchange services.

For more information about the NASA STI program, see the following:

- Access the NASA STI program home page at *http://www.sti.nasa.gov*

- E-mail your question via the Internet to help@sti.nasa.gov

- Fax your question to the NASA STI Help Desk at 443-757-5803

- Phone the NASA STI Help Desk at 443-757-5802

- Write to:
  NASA STI Help Desk
  NASA Center for AeroSpace Information
  7115 Standard Drive
  Hanover, MD 21076-1320

NASA/TM—2012–215995

Orion Pad Abort 1 Crew Module Mass Properties Test Approach and Results

Claudia Herrera and Adam Harding

Dryden Flight Research Center, Edwards, California

National Aeronautics and
Space Administration

Dryden Flight Research Center
Edwards, CA 93523-0273

March 2012

Available from:

NASA Center for AeroSpace Information
7115 Standard Drive
Hanover, MD 21076-1320
443-757-5802

Abstract

The Flight Loads Laboratory at the Dryden Flight Research Center (Edwards, California) conducted tests to measure the inertia properties of the Orion Pad Abort 1 (PA-1) Crew Module (CM). These measurements were taken to validate analytical predictions of the inertia properties of the vehicle and assist in reducing uncertainty for derived aero performance coefficients to be calculated post-launch. The first test conducted was to determine the Ixx of the CM. This test approach used a modified torsion pendulum test setup that allowed the suspended CM to rotate about the x-axis. The second test used a different approach to measure both the Iyy and Izz properties. This test used a knife-edge fixture that allowed small rotation of the CM about the y- and z-axes.

Discussions of the techniques and equations used to accomplish each test are presented. Comparisons with the predicted values used for the final flight calculations are made. Problem areas, with explanations and recommendations where available, are addressed. Finally, an evaluation of the value and success of these techniques to measure the moments of inertia of the CM is provided.

Nomenclature

CAD	computer aided design
CG	center of gravity
CM	Crew Module
CMLF	Crew Module Lifting Fixture
CMTF	Crew Module Transportation Fixture
DIM	Dynamic Inertia Measurement
DOF	degree of freedom
FBC	forward bay cover
FTAs	Flight Test Articles
GNC	Guidance, Navigation, and Control
IMU	Inertial Measurement Unit
KEF	knife-edge fixture
LaRC	Langley Research Center
LAS	Launch Abort System
LAV	Launch Abort Vehicle
LC	load cell
MOI	Moments of Inertia
MPET	Mass Properties Evaluation Tool
MPWG	Mass Properties Working Group
NASA	National Aeronautics and Space Association
PA-1	Orion Pad Abort
POI	products of inertia
SAWE	Society of Allied Weight Engineers
SepRing	Separation Ring
SRSS	square-root-of-the-sum-of-the-squares
TRR	Test Readiness Review
a	moment arms to spring attachment fixtures
d	air density
gc	gravity where load cell was calibrated
gm	gravity where measurement was done
h	vertical distance from test configuration CG to knife edge
Ixx	moment of inertia about the x-axis
Iyy	moment of inertia about the y-axis
Izz	moment of Inertia about the z-axis

k	spring stiffness
m	mass
M	corrected mass
$MeasuredMass$	measurement of mass
P	reference point
u	density of material displacing air
W	total weight of test configuration
X_{CG}	center of gravity location along the x-axis
y	moment arm from CG to spring attachment eyebolts
Y_{CG}	center of gravity location along the y-axis
Z_{CG}	center of gravity location along the z-axis
δ	spring plane angle
ω	frequency of oscillation in rad/sec

Background

In 2005 the National Aeronautics and Space Administration (NASA) began efforts to develop the next generation of manned launch vehicles capable of both low earth orbit and lunar-based missions. One of the first systems to be developed for this new space transport project was the Launch Abort System (LAS). This system would function similar to escape systems used on Apollo and Soyuz capsules. NASA's Dryden Flight Research Center (Edwards, California) was selected to take a significant role in the developmental launches of unmanned test capsules that would execute abort launches.

The first launch mission in these abort flight tests was a simulation of an Orion Pad Abort 1 (PA-1) launch. This mission focused on using the LAS to launch a boilerplate Crew Module (CM) on an escape trajectory away from the launch pad. The LAS would then separate, and the CM would briefly free-fall for 3.5 s before a system of parachutes would deploy to allow a moderated descent lasting 1 min and 50 s. The mass properties are used by the flight control system during the ascent and reorientation phases of flight. Additionally, because the CM would have no active flight control following separation from the LAS, it was critical to fully understand the mass properties of the CM. This motivated the requirement to determine by testing the moments of inertia (MOI) for the PA-1 CM at NASA Dryden.

The Flight Test Articles (FTAs) consist of three primary modules: LAS, which includes the nose cone, control motor, canard assembly, jettison motor, abort motor, and adapter cone; CM, which includes the parachute systems, and forward bay cover (FBC); and separation ring (SepRing) as shown in figure 1. Each of these units has a prescribed geometry.

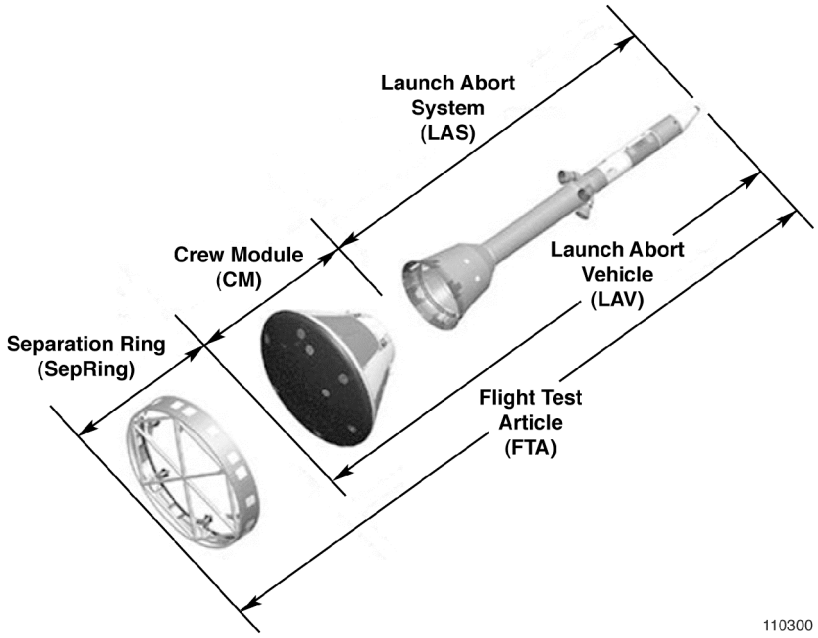

Figure 1. Flight Test Article configuration.

A brief introduction to the coordinate system used for the CM is shown in figure 2. The x-axis of the vehicle is along the longitudinal axis, positive aft "towards the vehicle" from the origin. The y-axis is positive toward the right-hand side of the seated crewmember. The z-axis is positive toward the head of the seated crewmember. This figure uses seated crewmembers for reference points only. The PA-1 crew module did not have actual seats installed.

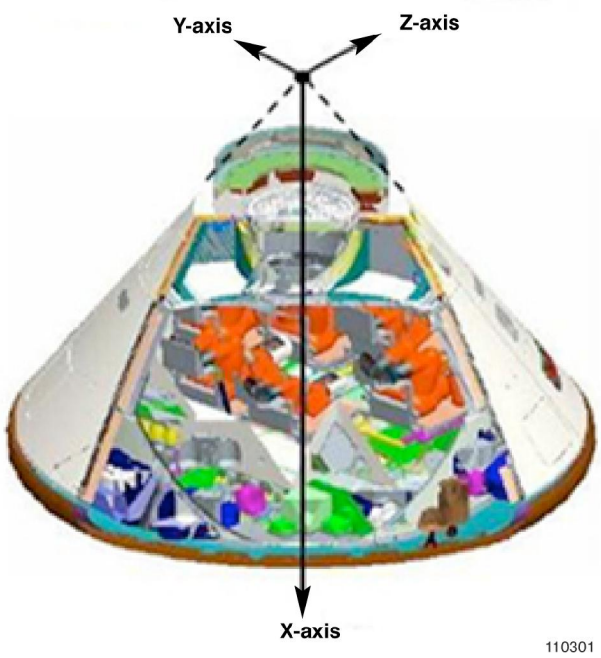

Figure 2. The PA-1 Crew Module Coordinate System.

Another customer of the measurement data from the testing at Dryden was the Mass Properties Working Group (MPWG) at NASA Langley Research Center (LaRC) (Hampton, Virginia). The MPWG was responsible for determining the proper ballast configuration of the CM. To accomplish this task it was decided to have both measured values and analytical predictions to use as a comparison. Additionally the MPWG had the option to use values from either measured values or analytical predictions in the final ballast calculations. The MPWG accomplished the analytical predictions by compiling a database to track installed item's mass contribution through weight tracking sheets and applying this data to organically developed tools to predict mass properties values and ballast solutions.

The mass properties values for the CM must fall within a given uncertainty range. The flight controls are certified to be able to control the vehicle when the actual center of gravity (CG) is within this envelope. Matching measured CG location to anticipated flight CG locations (or difficult to control CG locations) will be crucial to demonstrate proper flight dynamics of the Orion PA-1 Flight Test Article. Table 1 shows the desired range of uncertainty requirements from the disciplines of Guidance, Navigation, and Control (GNC) and Aero.

Table 1. Measurement uncertainty targets.

	GNC	Aero	Min
Mass (lbm)	+/- 30	+/- 30	+/- 30
X_{CG} (in)	+/- 0.5	+/- 0.5	+/- 0.5
Y_{CG} (in)	+/- 0.3	+/- 0.3	+/- 0.3
Z_{CG} (in)	+/- 0.3	+/- 0.3	+/- 0.3
Ixx (%)	+/- 5	+/- 3	+/- 3
Iyy (%)	+/- 10	+/- 3	+/- 3
Izz (%)	+/- 10	+/- 3	+/- 3

Brief Background on Mass Properties and Weight and CG

A brief introduction to the relationship of the mass and rotational inertia properties is of value prior to specific discussions of the development of methods and techniques. Newton's second law when expanded to the six degree-of-freedom (DOF) form to calculate all rigid body mass properties, the relation takes the form shown in figure 3, where *m* is the mass of the object, X_{CG}, Y_{CG}, Z_{CG}, are the locations of the CG measured from reference point *P*. The upper left quadrant provides the mass and is the most commonly and easily obtained measurement. The upper right and lower left quadrants provide CG location information. For aircraft, the most commonly measured is the X_{CG} followed by the Y_{CG}. The Z_{CG} is relatively more difficult to measure and not typically done. The remaining terms in the lower right quadrant of the mass matrix make up the inertia tensor. This quadrant is the most complicated to measure. Various pendulum methods have been developed to measure the diagonal terms or the moments of inertia, but are usually avoided due to the high cost and inherent high risk to the vehicle. The off diagonal terms of the inertia tensor (the products of inertia) are the most difficult to measure accurately by any known method.

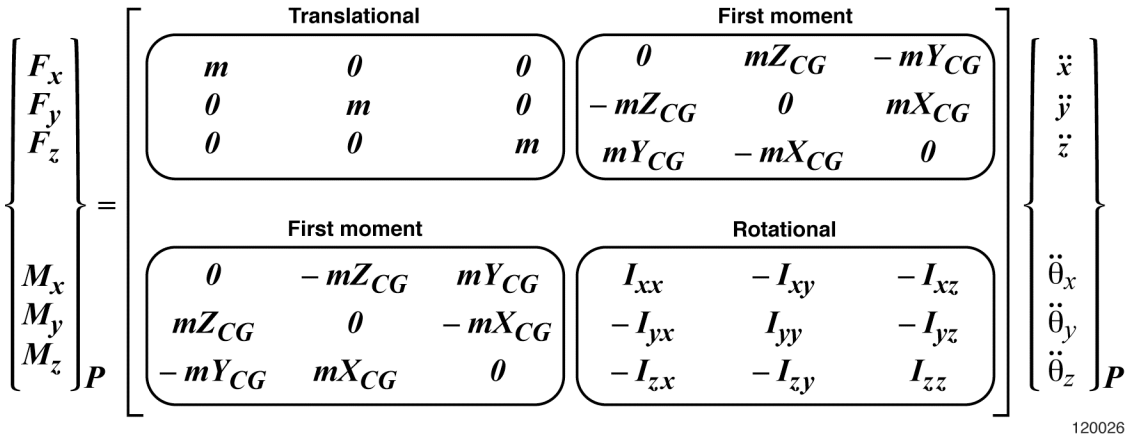

Figure 3. Newton's Law expanded to the 6-DOF mass matrix.

Tests to measure the weight, CG, and MOIs of the CM would provide data in direct support of several flight test objectives relating to dynamic stability. The primary objectives were to: (1) Demonstrate stability and control characteristics of the Launch Abort Vehicle (LAV) due to the LAS, and (2) Obtain data on the CM dynamic response during all parachute system sequences. The secondary objectives relating to dynamic stability were to: (1) Determine stability characteristics of the LAV configuration, (2) Determine the reorientation dynamics of the LAV, and (3) Determine the CM dynamic response to LAS jettison incorporating the aero performance coefficients (ref. 1).

Accurate mass distribution data is important to the flight test analysis. The mass characteristics relevant to rigid-body motions are weight, CG, and MOI. Moments of inertia and the vertical CG coordinate require specialized tests, which are an important part of the flight-test program.

Weight and Center of Gravity Testing Summary

Prior to performing the MOI testing on the PA-1 CM, the location of the capsule's CG needed to be determined to allow proper alignment with the CM's axis of rotation for each test. The typical industry standard for performing weight and CG measurements involves supporting the test article at three points, either suspended from above with cables or supported below, and taking weight measurements in several attitudes or tilt angles to determine vertical CG location.

For the PA-1 capsule, the decision was made to support the CM from below on three aircraft jacks. The jacks had load cells to provide the vertical force at the three jack positions that when summed equaled the weight of the CM. One at a time these jacks were used to tilt the CM to a specified angle. As the CM tilted, the weight distribution across the three jacks changed. Specific vehicle features (targets) and their orientations were tracked in 3D space, and this data along with the weight-deltas at each jack position was used to determine the CM's CG. A photo of this test setup is shown in figure 4. The Y_{CG} and Z_{CG} coordinates were determined by first moments using the load cell readings at all three known locations, while the CM was kept level. The vertical CG coordinate (X_{CG} in this case) was determined by the supported tilt method.

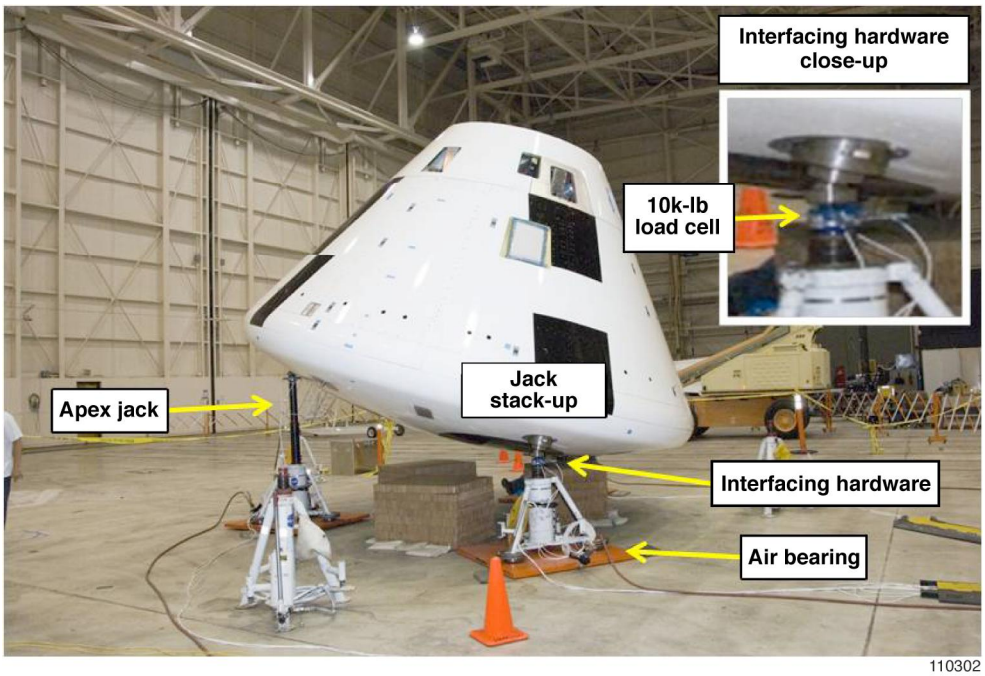

Figure 4. Weight and CG test setup.

Survey of Testing Methods for Determining Moments of Inertia

The preparation for the MOI testing began by reviewing the various established test methods and understanding the existing knowledge in this area. In order to calculate a body's moment of inertia about a particular axis, measurements of dynamic response such as oscillation period, rigid body acceleration, or torque around a rotation axis are taken. Values from these test results are then processed to calculate MOI. The majority of test methods measure the oscillation period of the body as it is rotated about the particular axis of interest. Often a restoring force such as gravity or a spring input is used in the test setup. Since the oscillatory methods were well documented, it was determined that focusing the literature review in this area would likely yield an experimental setup that would meet the constraints of the PA-1 CM. In addition to these traditional methods, investigation into a newer method, called the Dynamic Inertia Measurement (DIM) Method, was also explored. A brief summary of these two areas is presented with their unique benefits and challenges.

Oscillation-Based Test Methods

The classic methods of stable pendulum and inverted pendulum were noted to be widely used in MOI testing dating back to 1927. A summary table of these methods and their respective accuracies is presented in Appendix A, Summary of Experimental Accuracy for Inertia Test Methods. The stable pendulum methods include bifilar, trifilar, and simple pendulums as well as the torsion pendulum. This type of test-rig suspends the body of interest with the CG located in-between support filaments and below the pivot point. Then a force is applied to cause oscillation about the axis of inspection. The restoring force in this case is typically gravity. The period of oscillation is measured and used to calculate the body's MOI. A similar test approach uses an inverted pendulum, which measures the period of oscillation with the test subject and CG located above the pivot point of the test fixture. The restoring force is provided by springs in the inverted pendulum test-rig. The inverted pendulum is sometimes referred to as the knife-edge test method.

The review of historical test results reported the accuracy of the stable and inverted pendulum methods on the order of ±3 percent for many of the experiments. Evidence of higher error rates ranging from 10 percent to 20 percent, depending on the particular rotational axis and test setup, were also noted (ref. 2). There are two common sources of error that reduce the accuracy capabilities: mass effects of the fluid medium (air) and friction.

The contribution of additional mass from the buoyancy and entrapped air needs to be corrected and can typically contribute 1 percent error (ref. 2). Also, friction between the connections of the test setup such as the pendulum filaments and bearings provide a source of error due to additional damping. This contribution can be accounted for by measuring the free vibration response of the test fixture itself and subtracting the MOI contribution. Additionally there are several inherent sources of error specific to each type of pendulum setup.

The sources of error for the stable pendulum setup come from the filaments, the alignment of the test article, and the precession of the test object as it oscillates. The error source due to the filaments arises from the potential to have the filaments in a non-parallel configuration. If the distance between the top and bottom of the filament varies between filaments, the result will be a non-linear oscillation. The stable pendulum will always result in the CG aligning vertically under the filaments. If the CG is misaligned with respect to the axis of rotation, then the contributions from the products of inertia (POI) will contribute to the error. Being able to adjust the test hardware to align the CG under the filaments should be incorporated into the design. The third source of error is precession, which is when the test article is oscillating in two directions at the same time. This precession can result from either of the two factors previously mentioned in alignment or filament length. Also, precession can occur when the oscillation input force is applied to the test article. Carelessly applied forces will result in both rotation and translation of the test article and will contribute to error in the results (ref. 3).

The sources of error for the inverted pendulum arise from the use of springs, which supply the restoring force. The determination of the spring rate and ensuring the springs behave in a linear range during the test parameters will reduce erroneous influence from the springs in the results. If the springs are being used outside their linear range, the results will be more a demonstration of the influence of the springs than the response of the test article.

Dynamic Inertia Measurement Method

As observed by Mastinu et al. (ref. 4), there is an inherent obstacle to all of the "classical" oscillation-based testing methods requiring the vehicle (or body) to rotate around one axis. The orientation of the rotational axis must be changed with respect to the vehicle to determine the full inertia tensor. This potentially could lead to unique hardware and fixtures being designed and built for each axis to measure Ixx, Iyy, and Izz. A new method to estimate the inertia properties of a rigid body proposes a single test configuration that will provide data to calculate the entire inertia tensor (Ixx, Iyy, and Izz). This method is called the Dynamic Inertia Measurement (DIM) Method and has been in development at the University of Cincinnati on a variety of small scale test articles such as automobile brake rotors and steel blocks, as well as test fixtures native to the lab at the University of Cincinnati (ref. 5). In addition, NASA Dryden applied the DIM twice on the X-38 reentry vehicle (Scaled Composites, Mojave, California) between 1999 and 2001, which is of larger scale than previous rigid bodies. The DIM applies forces to an object and measures the resulting rigid body motion. This is done by using 6 DOF load cells, which measure support translational and rotational forces acting on the test article and a force transducer, which measures the excitation forces applied to the test article. Using an array of linear accelerometers to measure the 6 DOF acceleration of the test article; the mass, CG, and inertia tensor can be estimated (ref. 5). The DIM, when compared with the traditional oscillation-based methods, has several advantages of a more simplified setup and using a single test setup to replace 3 or 4 unique arrangements.

Selecting a Test Method

Following the survey of the various MOI testing techniques and compiling the requirements and potential sources of error, a down selection was made. The following discussion summarizes the rationale used in this selection process. The governing factors that influenced the selection were typical: cost, schedule, and test article constraints such as program requirements and the design of the test fixtures.

A significant impact to the selection of test approaches was the schedule constraints imposed upon the team. A delay in flight test hardware deliverables caused a shuffling of the schedule to recover lost time. Many of the activities planned for later in the schedule had to be moved earlier in the sequence. One of these activities was the

mass properties testing. Almost without exception the Mass Properties testing of flight vehicles is one of the very last tests performed prior to flight. This is because no matter how accurate the tracking efforts employed or how precise the predictions are, there is error in those predictions that only testing will be able to take into account. However, when the PA-1 CM Mass Properties were reprogrammed in the schedule, it moved from the final test prior to launch to before most of the major avionics equipment was installed. This meant that a large percentage of the final flight hardware mass would not be incorporated into the MOI tests.

Concern of the impact to the reliability of the data was expressed as a risk that was determined to be acceptable. This resulted in only four months to plan, design, and build test fixtures; and execute the tests on the capsule. Therefore plans for a fixture(s) capable of measuring all three MOI properties: Ixx, Iyy, and Izz would not have time to be designed and vetted. Instead, more simple structures and test fixtures would need to be used in the testing. There was also a significant level of resistance from the project to stay away from test fixtures that supported the CM in a 90-degree orientation. The change in the schedule made this point moot. A final schedule-related constraint on testing was the actual test window. There was only 10 working days available for all the mass properties tests, weight, CG, Ixx, Iyy, and Izz to be performed in a highly choreographed sequence that would not allow for retesting or rigorous data processing. This statement is not made to assign blame or distract from the results of the tests, but to set the background for the constraints that were imposed on the mission to measure the mass properties of the CM.

With the time constraint, at least two separate test fixtures would be needed to measure the Ixx MOI and then the Iyy and Izz properties. This gave the DIM approach an advantage over the classical methods with only requiring a single test configuration. However, the hardware (6-DOF force transducers) had a lead-time of 12 months. Also, the methods, procedures, and equations would need additional development time to be applicable to the CM. With the schedule constraints of the PA-1 launch, the DIM method would not have had time to mature.

The remaining options were all based on the oscillation methods. The choice was to either build an expensive fixture that would be able to suspend the CM in three configurations for all three MOI tests or build two different fixtures, one for Ixx and one for Iyy and Izz. The preliminary design and cost estimates for the single fixture is projected to consume more funding and schedule than two more simple fixtures. The bifilar method posed potential additional hardware that would need to be designed, so the decision was made that a simple torsion pendulum could determine the Ixx property and be done using the CM Lifting Fixture (CMLF) and a crane. A different test setup of an inverted pendulum fixture would provide both Iyy and Izz. The inverted pendulum was selected since it would allow the CM to be supported at three of the six jack points. Thus no additional lifting hardware would need to be designed. The next sections will summarize the setup for each test.

Developmental Testing

Once the test methods were decided upon, several developmental tests were conducted to further refine the methods, procedures, safety requirements, and data reduction prior to the actual testing of the CM. The initial testing to develop the weight and CG procedures used a flat steel plate measuring 4 ft x 4 ft x 2 in. and weighing approximately 1,400 lb. The simple geometry of the flat plate allowed the exact CG location of the steel plate to be calculated serving as a check for the measured values. Once the procedures and tests were conducted on the flat steel plate, the second phase of developmental testing used a full-scale mockup CM that weighed approximately 4,000 lb. The mockup CM was constructed from aluminum beams and aluminum sheets that approximated the major structural elements of the actual CM. The Weight and CG tests procedures were again conducted on the mockup CM to further develop the procedures. This testing was beneficial in uncovering challenges such as how to move the aircraft jacks during tilting operations and how to use the laser trackers to monitor the predetermined targets on the CM.

When the developmental tests were complete the lessons learned were incorporated into the final test plans and procedures used for the testing of the flight hardware. This was seen as an excellent risk reduction effort that

identified hazards and ways to mitigate them without putting the actual CM at risk of damage. Following a final Test Readiness Review (TRR) of the weight and CG procedures, approval was granted to test the actual CM. Developmental testing for the Ixx, Iyy, and Izz procedures were not as in depth and did not use the mockup CM due to the fact that the CM would remain nearly level during these procedures. There also was no time remaining for additional MOI developmental testing with the mockup CM. While this was acceptable from the standpoint of safety and risk to the flight hardware, it would have been beneficial to use the mockup CM in the MOI testing to have time for post-test data reduction development.

Weight and CG Setup

The first data taken for the mass properties testing was of the weight of the CM. This weight measurement was done using the CMLF, a 25,000-lb load cell, and a crane. The crane would lift the CM off the CM Transportation Fixture (CMTF) to allow an inch of clearance. The weight would be recorded and the procedure would be repeated two more times. All lifting hardware or hardware added only to perform this measurement was weighed separately to be removed from the CM load cell measurements.

The CM was lifted off of the CMTF and placed on three aircraft jacks. The three aircraft jacks were adjusted to account for unevenness in the floor and jack stack-ups in order to achieve a level CM configuration. The vertical CG test required the CM to be tilted by extending a jack to change the weight distribution across the three jacks. Each of the jacks was extended separately to evaluate the repeatability of the measurement. Figure 4 shows the CM in a tilted orientation. These jacks had a 10,000-lb load cell positioned between the jack and the CM allowing the weight at that position to be measured. This required the extended or "apex" jack to be translated in towards the center of the CM. To allow for this translation, air pallets were positioned underneath each aircraft jack to provide freedom of motion in the X-Y plane of the hangar floor. Values for the weight at each position were recorded at predetermined jack heights. This testing method is shown in figure 4.

Ixx Test Setup

The torsion pendulum took advantage of the CMLF that was already fabricated and approved for lifting the CM. A crane suspended the CM using the CMLF, and a pair of attachment lever arms was added to the base of the CM at the 0 and 180 degree locations. These arms extended horizontally to a set of calibrated springs that were pre-loaded and set a desired spring plane angle. A diagram of this test arrangement is shown in figure 5, and figure 6 shows a photograph from the actual testing. The input force was applied at one extension arm, and the test article was allowed to oscillate about the x-axis. Measurements were taken using two laser trackers, an Inertial Measurement Unit (IMU) and string pots that tracked the 3 dimensional position and rotational rate of the CM.

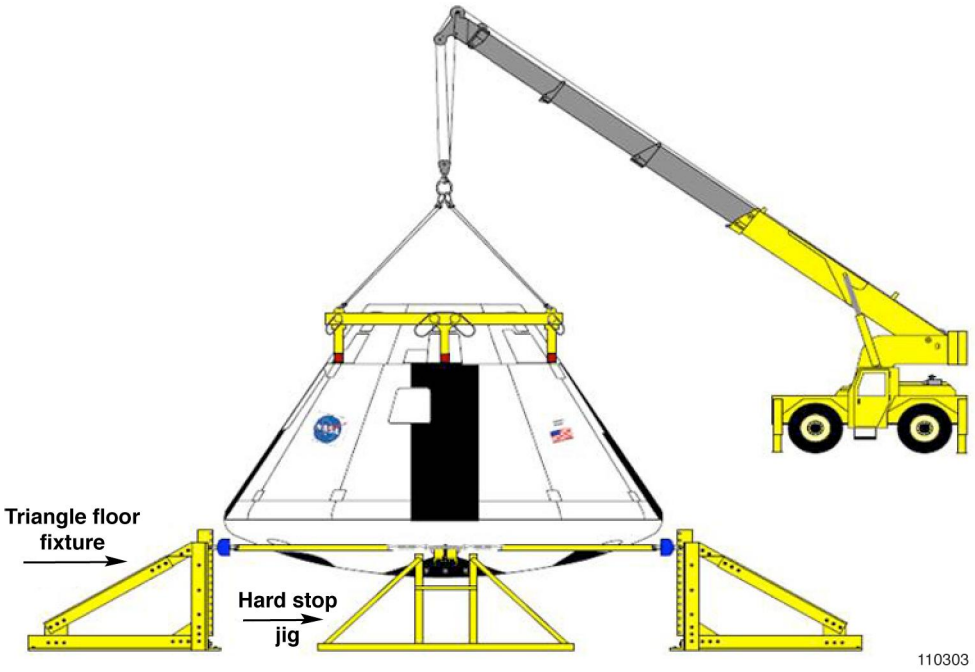

Figure 5. Torsion pendulum test configuration for Ixx.

Figure 6. Torsion pendulum test setup at the Flight Loads Lab at NASA Dryden.

Iyy/Izz Test Setup

The test arrangement to measure the rigid responses used in calculating the Iyy and Izz MOIs used the inverted pendulum method. This required the design and fabrication of a test fixture that would support the CM

from the attachment points on the heat shield and then pivot along a “knife-edge” axis, in one configuration about the y-axis and one about the z-axis. The restoring force was provided by calibrated springs in tension. Laser trackers and string pots tracked position data. The change between the Iyy configuration and the Izz configuration required lifting the CM and rotating it 90 degrees. Once the CM was installed onto the knife-edge fixture, ballast was added to balance the entire setup. Once the tension in the springs was equal, the supporting jacks were lowered at the four corners of the fixture, and the CM and fixture were free to oscillate or rock back-and-forth with about ±1.5 in. of amplitude. A figure and photo documenting this test setup are shown in figures 7 and 8, respectively.

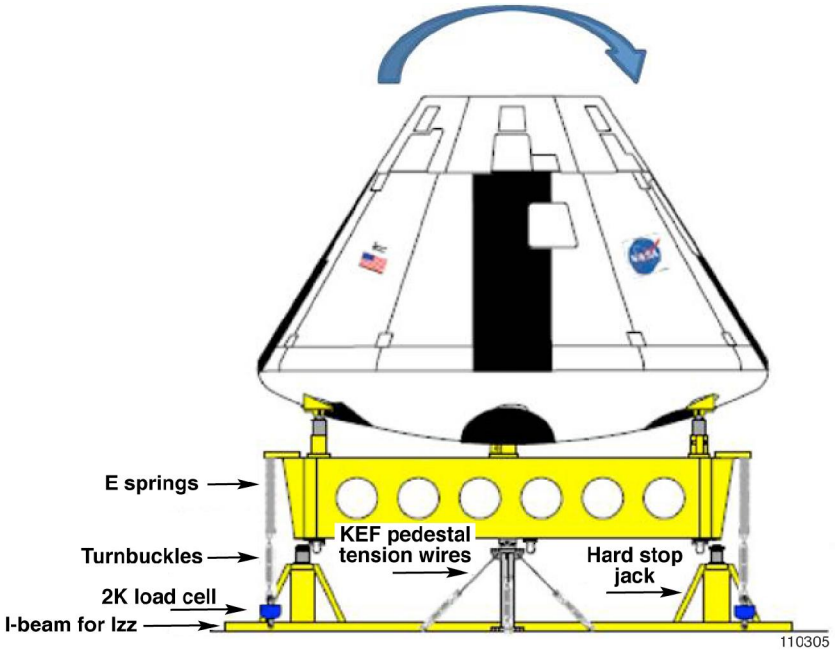

Figure 7. Iyy/Izz test setup.

Figure 8. Iyy/Izz test setup in the Flight Loads Lab at NASA Dryden.

Analysis Approach

The approach to analyzing the test data was derived from the requirement for high accuracy based on best practices from the Society of Allied Weight Engineers (SAWE) and industry best practices (ref. 6). The analysis approach for all testing methods employed is discussed as well as any considerations for error or data corrections.

Corrections and Sources of Error

There are many contributions of error that are sometimes considered negligible, depending on the application and the measurement uncertainty requirements. In this case, however, it was imperative to obtain highly accurate data. Therefore, the error from these sources was quantified in an effort to reduce measurement error. The following sections describe these contributions, how they were measured, and how they were accounted for when processing the data for each of the test methods.

Load Cell Reading Corrections

Two corrections to load cell measurements were performed to acquire more accurate load cell data. These adjustments were performed per SAWE handbook guidance (Ref. 6). The first correction was performed to acquire a more accurate load cell reading using the load cell calibration curve. This correction was done by taking the load cell voltage output and inputting it in the equation corresponding to load cell response based on a 10-point calibration. The second correction was performed to account for differences in gravity between the load cell calibration site and actual load cell application site. Equation (1) was the equation used for this correction:

$$M = \frac{g_c \times MeasuredMass}{g_m} \tag{1}$$

where g_c equals gravity where load cell was calibrated, g_m equals gravity where measurement was done, *Measured Mass* equals measurement of mass, and M equals corrected mass. Gravity values were obtained for both locations and this correction was implemented in the data processing. These two corrections had an effect of increasing the CM mass by 0.035 slugs.

Air Buoyancy Correction

Another recommended adjustment when measuring the mass of an object was to account for buoyancy effects from the surrounding air (ref. 7). This correction required having a weather station at the test site and recording the ambient conditions at the time load cell data was recorded. These data were used to calculate the in situ air density during the weight and CG measurement. Per standard practice, using this equation required knowing the amount of volume that gets displaced by the CM and an analytical mass estimate of each material of the test article (ref. 8). These mass and volume values were estimated based on a detailed computer aided design (CAD) model. A density was calculated for all the material displacing air and then used in equation (2). The air buoyancy correction increased the CM mass by 0.366 slugs. Equation (2) is:

$$TrueMass = MeasuredMass \times \left(1 + \frac{d}{u}\right) \tag{2}$$

where d equals air density, and u equals density of material displacing air.

Definition of Level

A tolerance on the levelness of the CM was applied for practical purposes. Based on initial uncertainty analyses, the requirement was to level the CM to within +/- 0.010 in. as verified by a laser tracker. As the test was being conducted, it quickly became apparent that this requirement was very time consuming. The requirement

was updated to +/- 0.100 in. A table was developed to correct the calculated CG for any bias contributed by the CM deviating from a level state. Figure 9 shows the error that is introduced when the CM Y-Z plane is not perpendicular to the gravity vector.

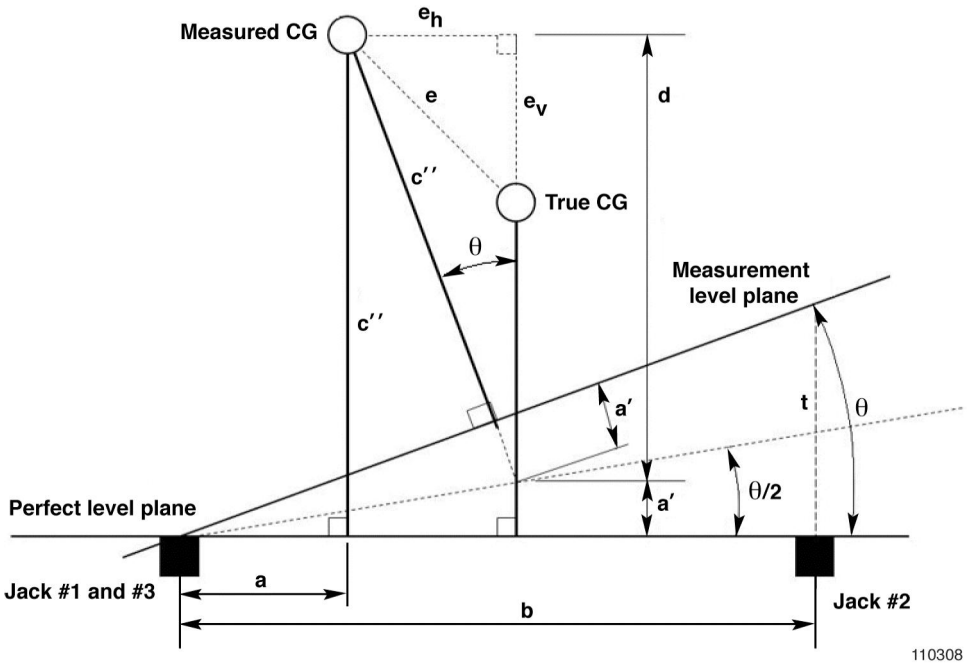

Figure 9. Error introduced by a non-level CM configuration.

When the measurement level plane was tilted, the measured CG was shifted from the true CG. The tilt was caused by allowing a small difference (t) to exist between the minimum and maximum X coordinates of any 3 data points. Usually this difference (t) was a very small number. The lengths (c) and (c') did not change, but the measured CG height (c") was calculated above the perfect level plane. This height (c") was in error by the vertical bias error called (e_v). Also the shifting of the CG created a horizontal bias error (e_h). The total bias error (e) was calculated by combining the errors (e_v) and (e_h) via the square-root-of-the-sum-of-the-squares (SRSS) of the two values. The CM measurement level plane angle was measured with a laser tracker and then used to adjust the measured CG values if necessary. However, it was found that by limiting t to 0.100 in., the error in the measured CG was less than 0.010 in.; and therefore, negligible.

Considerations Regarding Side Loads

The load cells incorporated in the jack stack-ups were 10,000-lb tri-axial load cells. They measured vertical load and side loads as moments for both the X and Y directions relative to the local load cell coordinate system. Measuring three components of the support load was considered unconventional, and there were various discussions regarding the implications of measuring these side loads. Initially, the side loads were going to be used as a monitoring tool only. The side loads would be considered an indication of misalignment between the ball and cup center points. Adjustments would serve to improve jack alignment and decrease side loads when they exceeded a certain value. Going into the test, the not-to-exceed side load value was set at a tolerance that was considered small enough to not affect data quality. The side load was allowed to reach 100 lb before an attempt to align the jack stack-ups was made. The air pallets were expected to help alleviate the issue of high side loads. In practice, this concept was not successful. The air pallets did not alleviate the side load issue as much as expected, and the jacks were difficult to adjust. High side loads were an inherent part of the measurements. The side load limit was then expanded to reflect the structural limitations of the jack stack-up hardware and was set to 500 lb. Because the data would have a side load component, a variety of methods were evaluated on how to account and correct for this in the final CG calculations. The accepted approach was to consider a high side load as increased

uncertainty in the vertical load reading. These load cells possess a 1 percent cross talk rate, which is the uncertainty (for multi-axis load cells) where mechanical coupling between the mutually perpendicular sensing axes can affect the output of the primary axis. One percent of the side load would be added to the uncertainty in the load cell reading for the vertical load. For example, a 400-lb side load increased the uncertainty in the load cell vertical load reading by 4 lb. A higher side load was considered to indicate a less precise vertical load cell reading. In this way, the side load was included in the uncertainty analysis aspect of the results as described in the Uncertainty Analysis Section.

Weight and CG Analysis Approach

The weight of the CM was measured using two methods. The first method consisted of suspending the CM and including a 25,000-lb capacity load cell in the lifting train. The process for calculating the mass of the CM from this measurement was as follows:

1. Obtain a CM weight using 25,000-lb load cell.
2. Obtain a lifting train weight using 2,000-lb load cell.
3. Obtain any miscellaneous hardware weight using a 50-lb capacity bench scale.
4. Perform load cell corrections.
5. Remove tare weight from measurement.
6. Convert to mass.
7. Perform buoyancy correction.

The three-point support method was the second method used to measure weight. In addition, this was the method used to measure CG location. The jack stack-up interfacing hardware was weighed on the bench scale and removed from the total sum of all three load cell readings. This second sequence for calculating the weight of the CM was as follows:

1. Obtain load cell readings from all three load cells.
2. Perform load cell corrections.
3. Summate all load cell readings.
4. Obtain any interfacing hardware weight using a bench scale.
5. Remove tare weight from measurement.
6. Convert to mass.
7. Perform buoyancy correction.

This method was also used to calculate the Y_{CG} and Z_{CG} locations by leveling the CM and then taking load cell readings, and recording their locations using a laser tracker. Equation (3), the equation for calculating a CG for the CM in the test configuration was as follows:

$$\text{Test Configuration } \bar{z}, \bar{y} = \frac{\sum (LC \times coord)}{\sum (LC)} \tag{3}$$

where *LC* is the load cell reading and *coord* is the Y or Z coordinate of the center of the load cell.

The test setup was then re-configured to use a supported tilt method to calculate the X_{CG} (Ref. 9). The approach for calculating X_{CG} is based on the re-distribution of CM weight as the geometry changes. The CM was tilted through an angle of 18 degrees by extending the apex jack. The apex jack was translated in (towards the fixed jacks) using an air pallet. The differences in the load cell readings from level to tilted conditions were used to measure the X_{CG} location. Figure 10 shows the method described.

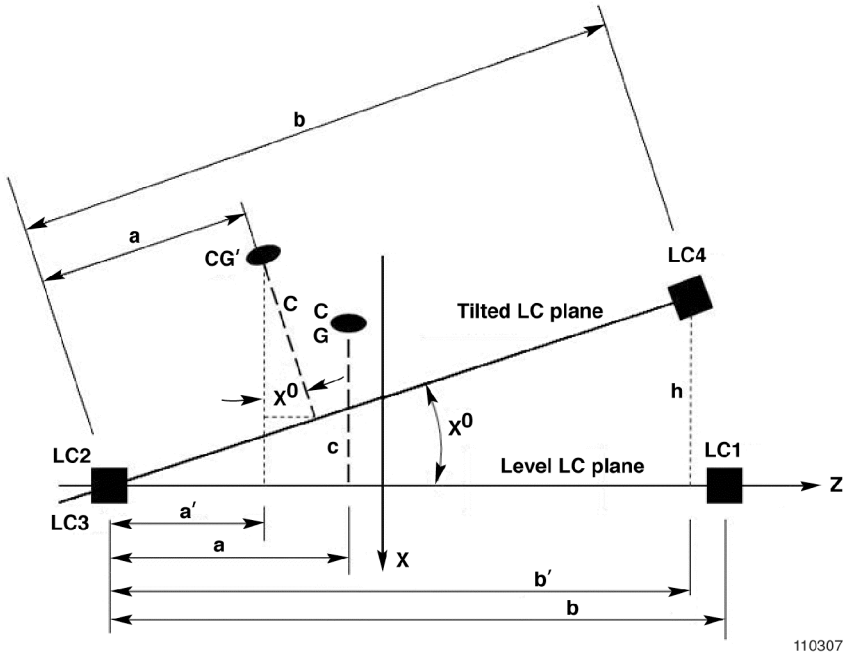

a = length between fixed load cells and CG when load cell plane is level and parallel to Z axis.
a′ = length between fixed load cells and CG′ when load cell plane is tilted by angle X^0.
b = length between fixed load cells and apex load cell when load cell plane is level.
b′ = length between fixed load cells and apex load cell when load cell plane is tilted by angle X^0.
LC1 = apex load cell, located on jack that is extended to tilt CM.
LC2/LC3 = fixed load cells, located on jacks that are stationary during tilting.
LC4 = re-position of CL1 after load cell plane is tilted by angle X^0.
M = total weight of CM at CG or CG′ in any configuration.
W = total combined weight of fixed load cells when load cell plane is level.
W′ = total combined weight of fixed load cells when load cell plane is tilted by angle X^0.
X^0 = angle of tilt.
h = height of tilt, vertically at LC4.
c = height of CG or CG′ above level load cell plane, distance above the plane does not change.

Figure 10. X_{CG} measurement setup.

Equation (4) applied to this method is:

$$c = \frac{\left[\left(b \times b'\right) \times \left(W' - W\right)\right]}{h \times M} \tag{4}$$

This measured CG rendered the value for *c*, which is a measure of the vertical distance of the CG to the load cell plane. This was converted to the CM coordinate system to obtain a test configuration X_{CG} value.

The CG locations calculated corresponded to the test configuration of the CM, which included the test fixtures necessary to interface the CM heat shield to the jack stack-ups. The weight and CG of the test hardware was obtained and used to calculate the CM CG location. Equation (5) was used to extract the CM CG from the test configuration CG, which is a combination of CM and test fixtures:

$$cg = \frac{\left[CG_{Comb} \times \left(Mass_{Fixt} + Mass_{CM}\right)\right] - \left[CG_{Fixt} \times Mass_{Fixt}\right]}{Mass_{CM}} \tag{5}$$

Various corrections and adjustments were evaluated and performed during the processing of the CG data. The process for calculating the CM CG from the test configuration CG was as follows:

1. Obtain load cell readings from all three load cells.
2. Perform load cell-reading corrections.
3. Calculate test configuration CG.
4. Calculate CM only CG.

Torsion Pendulum – Ixx Analysis Approach

The torsion pendulum method was used to measure the CM inertia about the x-axis. The frequency of the oscillation was measured using load cells, string pots, an IMU, and the laser tracker. Distance from the test article CG to the point of application of the restoring force is another parameter for calculating the inertia. This moment arm was measured using the laser tracker. The final parameter to identify is the spring plane angle (δ). The spring plane was the plane created by all four springs. The spring plane was inclined through several angles (δ) to measure Ixx and Ixy. The angle was changed by attaching the spring stack-ups at different locations on the triangular posts. Equation (6) shows how *Ixx* was calculated for the combined test article, meaning CM, CMLF, and other test hardware,

$$\text{Measured } Ixx_{comb} = \frac{y^2 \times \sum[k] \times \cos(\delta)}{\omega^2} \tag{6}$$

where, y = moment arm from CG to spring attachment eyebolts, k = spring stiffness, δ angle = angle of spring plane inclination, and ω = frequency of oscillation in rad/sec.

To obtain the cross product of inertia, the pitch-to-roll ratios are plotted as a function of the spring plane angle. The spring plane angle where the pitch-to-roll ratio crosses the zero value was the angle used in Equation (7) to calculate *Ixy* using *Ixx*.

$$Ixy = Ixx \times \tan(\delta_o) \tag{7}$$

As with the weight and CG tests, the result of this test measured a mass property for the test article, which included a significant amount of test fixtures. A separate torsion pendulum test was done to measure the CG and *Ixx* of the CMLF and spring attachment arms such that their contribution could be removed from the measured value of the combined test article using the parallel axis theorem. Equation 8 shows how test fixtures contribute to the measured value of the combined test article.

$$\text{Measured } Ixx_{comb} = Ixx_{CM} + \left(CMonly\_mass \times d_{CMcg}{}^2\right) + Ixx_{Fixt} + \left(Fixt\_mass \times d_{Fixtcg}{}^2\right) \tag{8}$$

Knife Edge – Iyy/Izz Analysis Approach

The knife-edge method was used to measure the moment of inertia about the y- and z-axes. The frequency of the oscillation was measured using load cells in the spring stack-ups, string pots, an IMU, and the laser tracker. Other test setup parameters for calculating the inertia were the distances from the test article CG to the point of application of the restoring forces, test article weight and vertical distance of CG to knife edge. All distances were measured with the laser tracker. Equation (9) was used to calculate the combined test article about the y- and z-axes using the knife-edge method,

$$\text{Measured } I_{comb} = \frac{\left[\left(k_1 + k_2\right)a^2 - \left(W \times h\right)\right]}{\omega^2} \tag{9}$$

where, a = moment arms to spring attachment fixtures, k = spring stiffness, W = total weight of test configuration, h = vertical distance from test configuration CG to knife edge, and ω = frequency of oscillation in rad/sec.

Similar to the *Ixx* measurements, the inertias measured included a significant contribution from the test fixtures. A separate test was done to measure the weight, CG, *Iyy*, and *Izz* of the knife-edge fixture and other test fixtures to extract a set of CM only inertia values (eq. (10).

$$\text{Measured } I_{comb} = I_{CM} + \left(CMonly\_mass \times d_{CMcg}{}^2\right) + I_{Fixt} + \left(Fixt\_mass \times d_{Fixtcg}{}^2\right) \tag{10}$$

Other Considerations for Oscillation-based Test Methods

Other factors were considered when analyzing inertia calculations; namely air mass effects and damping effects. Air mass effects were estimated based on CM geometry and considered to be negligible. Damping effects were not taken into account based on SAWE criteria for selecting frequency measurements where change in amplitude per cycle was decreased by less than 10 percent (ref. 4). Ten to twenty oscillations that satisfied this requirement were averaged for frequency calculation (ref. 9).

Ballast was used during the knife-edge testing to minimize the effort needed to attain a level test article configuration. This ballast was in the form of solid discs. Their weight was well known and their location was measured with high precision using the laser tracker to enable the removal of their contribution.

Results and Discussion

Values for the desired mass properties values were calculated using the analysis approach previously described. Those values are presented in the following sections. In addition, the analytical values for those mass properties are also presented and compared to test results. Finally, an uncertainty analysis was done for each measured value.

Analytical Predictions

Analytical predictions were derived by the NASA LaRC contingent of the Orion PA-1 MPWG. NASA LaRC developed a tool referred to as the Mass Properties Evaluation Tool (MPET). It is an analysis code that supplements a detailed CAD model, with actual weight measurements and weight growth allowances. It was used to model, track and update with actual measurements, and report analytical predictions for the mass properties of the Orion PA-1 CM. This tool is discussed in further detail in reference 10.

Test Results

The mass of the CM was measured using two methods. Five mass measurements were performed on the CM using the suspended method, and six mass measurements were performed using three point support method. The values between the two methods differed by about 1.087 slugs (35 lbm). It was decided to accept the mass measured with the three-point support method as the mass value to report since it corresponded to the CG measurements. Six measurements for the Y_{CG} and Z_{CG} were performed. These results correlated relatively well with the value predicted by the MPET (ref. 10). Lastly, the method used for measuring X_{CG} proved to render unreliable results at low angles of tilt. The maximum tilt height was limited to 18 degrees by the jack extension

available (33 in.). The more reliable measurements were produced by tilt heights of 25 to 33 in. This is discussed further in the Uncertainty Analysis section.

The inertia measurements did not correlate as well as the mass and CG test results did with the respective analytical values. The torsion pendulum result matched the predicted value relatively well, while the uncertainty in the measurement well exceeded the uncertainty target for this parameter. The CM possesses six interface points that attach to the SepRing. Because of time constraints, the project was limited to using the interface points at the 0 and 180 degree locations rather than designing and fabricating inertia testing hardware that could allow the use of other locations. Because of the locations of these interface points relative to the CM coordinate system, it was only possible to attempt to measure the Ixy product of inertia term. However, the Ixy value for the CM at test configuration was very close to zero, and therefore, a reliable measurement of this property using the chosen method was not possible.

The Iyy/Izz knife-edge testing provided a different set of challenges. The testing data showed large variations in oscillation frequency within a single test run time history. Because this frequency term is squared in the calculation of inertia, this method is highly sensitive to variation in frequency. Frequencies varied by as much as 10 percent from beginning to end of a time history. Testing results comparison to MPET values ranged anywhere from 0.5 percent to 46 percent depending on how the frequency data was analyzed. The source of this strong non-linearity is from the vertical distance of the combined CM/knife-edge fixture CG to the knife-edge pivot axis (ref. 11), the *h* term. Based on X-38 implementation of this method and considerations presented in reference 11, it was not expected to dominate as much as was observed. It was also expected that this effect could be minimized if oscillations were kept to a small angle (+/-2 degrees), which was not the case. The linear assumption of the system could not account for this non-linear contribution by the *h* term. In comparison to the X-38 and the lifting body, which possessed an *h* term in the 40-inch range, the CM *h* term was 80 in. Conversely, the inertia testing of the knife-edge fixture by itself, where the *h* term was about 15 in., rendered better oscillation data and gave a variation of about 1 percent. However, due to the large variations in the CM inertia results, the program decided to use the MPET predicted values in analyses requiring mass property values.

Uncertainty Analysis

The program provided measurement uncertainty targets, which determined the tolerances on the setup and instrumentation. An uncertainty analysis was performed for each test method based on setup, equations used, and instrumentation sensitivity. This was also done for the variation actually observed in the measurements.

The weight and CG measurement sources of uncertainty included the load cells, the bench scale, the CG location estimation for the test fixtures, and the laser tracker measurements. The usage of 3-DOF load cells for weight and CG measurements had not been previously attempted. The original objective was to use the lateral axes as an indication of alignment, which would indicate a need for adjusting the supports to provide better vertical load readings. This method was effective during the developmental testing. However, though the mockup CM resembled the flight CM in dimensions and shape, it was only 1/3 of its tested weight. Due to the heavy load and the floor not being smooth enough to allow air bearings to function properly, the system was unable to adequately adjust the supports, and side loads were greater than expected. There is no proven method for incorporating these measured side loads into the weight and CG calculations, and an extensive testing effort would be required to derive a process. Alternatively, different sets of interfacing hardware designs should be evaluated for safety and effectiveness at minimizing side loads. Suspending the test article at three points would greatly reduce side loads. However, that method possesses other challenges of implementation. The determination was made to increase the uncertainty in the vertical load as a function of side load magnitude. These load cells possess a cross talk rate of 1 percent; therefore, 1 percent of the side load was added to vertical load cell uncertainty. The total uncertainty in the load cell data included uncertainty from the data acquisition system, the load cell accuracy, and side loads present during measurement. The uncertainties assigned for this instrumentation are listed in table 2. Though test results agreed with analytical results, weight and CG measurement uncertainties

exceeded the target measurement uncertainties. The hardware, instrumentation and test setup did not possess the fidelity to satisfy the target uncertainties.

Table 2. Weight and CG uncertainty values.

Sensor	Uncertainty	Unit
2k-lb load cell	1.870	lbf
25k-lb load cell	23.700	lbf
10k-lb load cell	9.380	lbf
Test hardware CG location – CAD	0.010	in.
50-lb bench scale	0.020	lbf
Laser tracker	0.003	in.

In addition to high side loads, the X_{CG} measurement uncertainty was affected by the angle of tilt. Load cell data taken at tilt heights less than 25 in. (15 to 20 in. heights) produced a change in load that was less than 1,000 lb (10 percent of load cell capacity). Results show a large scatter (2 in.) for these low tilt heights. Measurements taken at 25 to 33 in. of jack extension were used in calculating the CM X_{CG} location. By the sine of tilt angle, it is clear that higher tilt angles provide better data, with the best results achieved when the longitudinal axis is horizontal, and the test article is suspended using a bifilar setup.

Several issues arose during Ixx testing, which could have increased measurement uncertainty. The crane used to suspend the CM was a mobile crane with a hydraulic system, which experienced drift as testing progressed during the day. Though the crane boom was adjusted to minimize this drift, it is unknown what effects this had on the data or how much better an overhead crane would have served in Ixx testing. Another potential source of error was the straps used to suspend the CM from the CM lifting fixture. Though the fixture was rigid, these straps were not and the effects of the participation of their flexibility in the torsional pendulum are unknown. The uncertainties in the Ixx calculation for the CM came from the string pots, the laser tracker, the spring stiffness, the spring moment arms, the ability to measure frequency of oscillation, and the ability to measure the CG of the CM Lifting Fixture (table 3).

Table 3. Ixx uncertainty values.

Sensor	Uncertainty	Unit
42-inch string pot	0.023	inches
Spring stiffnesses	5.000	lb/ft
Spring moment arms	0.250	in.
Frequency	0.040	rad/sec
CM weight - measured	28.000	lbf
CM CG - measured	0.352	in.
CM lifting fixture CG – measured	0.160	in.
CM lifting fixture weight - measured	0.440	lbf
Laser tracker	0.003	in.

The Iyy/Izz testing proved to be the most challenging in terms of acquiring trustworthy data. The frequency data exhibited large variations and large changes in amplitude (meaning high damping). Furthermore, the knife-edge testing method sensitivity to the *h* term, and its large magnitude for this test article, severely affected the validity of the data. Sources of uncertainty and their value are listed in table 4.

Table 4. Iyy/Izz uncertainty values.

Sensor	Uncertainty	Unit
6-inch string pot	0.011	in.
Spring stiffnesses	5.000	lb/ft
Spring moment arms	0.250	in.
Frequency	0.040	rad/sec
Knife-edge fixture CG – measured	0.440	in.
Knife-edge fixture weight - measured	5.200	lbf
Laser tracker	0.003	in.
Frequency	0.040	rad/sec
CM weight - measured	28.000	lbf
CM CG - measured	0.900	in.
Spring plane angle	1.340	deg

Test versus Analysis

The following sections present the results of all these tests and how they compared to predicted values. These test results represent values for the CM in the mass properties testing configuration and not final flight configuration. The MPET values are also presented as a comparison, and the difference is calculated and presented as the delta. The uncertainty calculated for each measurement is shown as well. The test results, analytical values, deltas between test and analytical values, and the uncertainties associated with each test result are given in table 5.

Table 5. Analytical versus test results.

	Mass (slugs)	Mass (lbm)	X_{CG} (in)	Y_{CG} (in)	Z_{CG} (in)	Ixx (slug-ft^2)	Iyy (slug-ft^2)	Izz (slug-ft^2)
MPET	395.688	12,730.88	750.080	0.220	-1.990	9,200	9,520	9,620
Test	400.758	12,894.00	750.990	0.163	-2.158	9,700	5,140	5,520
Uncertainty	0.870	28.00	0.810	0.129	0.352	290	2,200	2,500
delta	5.070	-163.12	-0.900	0.060	0.170	-500	4,380	4,080

Lessons Learned and Recommendations

There were lessons learned across all methods used for measuring the mass properties of the command module. They are listed by test method as follows:

1. General
   - A build-up approach to become familiar with test procedures is a good practice.
   - Practice tests should be performed with a test article as similar to the actual test article as possible.

2. Weight and CG
   - An extensive set of tests would help evaluate how to implement side load measurements in weight and CG calculations.
   - When using a 3-point support method, interface design should minimize side loads in load cell readings.
   - When using air pallets, the smoother the floor, the greater their effectiveness.
   - If possible, a 3-point suspension method should be used.
   - When using a tilt method to measure longitudinal CG, high angles are needed.
   - Ensure all measurements are at least at 10 percent of the full measurement range of the sensor at all test configurations.
   - A longitudinal CG is best measured by suspending the test article using a bifilar setup with load cells in the lifting trains.
3. Torsion Pendulum Testing - Ixx
   - An overhead crane works better than a mobile crane whose boom will drift over time.
   - The test fixture should be as rigid as possible.
   - An IMU with adequate sensitivity should be used to measure the rate of oscillation.
   - Setup is not sensitive enough to measure a near-zero cross product term. Orienting the test article differently would have allowed for a better measurement of a cross product of inertia.
   - As much real-time evaluation of data should be performed as practical.
4. Knife-Edge Testing – Iyy/Izz
   - Vertical distance from test article CG to knife edge should be minimized based on acceptable error in the measurement.
   - The test fixture should be as rigid as possible.
   - An IMU with adequate sensitivity should be used to measure rate of oscillation.
   - As much real-time evaluation of data should be performed as practical.

Conclusion

Various tests were conducted in fall of 2008 to measure the mass properties of the Orion PA-1 Command Module. A three-point support method was used to measure weight and CG, with a tilt configuration for X_{CG} measurement, a torsion pendulum to measure Ixx, and a knife-edge setup to measure Iyy and Izz. All test methods had challenges associated with meeting the target measurement uncertainties prescribed by the program. Though in some cases the measurements matched the predicted values relatively well, measurement uncertainties were not acceptable. However, because there was some degree of correlation in the weight and CG analytical and test values, there was a higher level of confidence in the analytical inertia values. There was a broad range of lessons learned that could help improve the overall quality of the results of these types of tests in the future.

Appendix A

Summary of Experimental Accuracy for Inertia Test Methods

					Reported Accuracy (+/- %)			
Article	Title	Author	Date	Method	Ix	Iy	Iz	Notes:
Tech note 2201	Measurement of the moments of inertia of an airplane by a simplified method	H. L. Turner	1-Oct-50	Knife-edge	1.7	1.2	0.6	Reference made to tech note 1629.
Tech note 3084	A method for measuring the product of inertia and the inclination of the principal longitudinal axis of inertia of an airplane	Boucher, Rich, Crane, Matheny	1-Apr-54	Knife-edge	0.92 1.0	0.48 0.49	0.35 0.35	Load Condition #1. Load Condition #2.
Tech note 1629	The experimental determination of the moments of inertia of airplanes by a simplified compound-pendulum method	W. Gracey	1-Jun-48	Bifilar	2.5	1.3	0.8	Same numbers in tech note 467.
Tech note 351	An accurate method of measuring the moments of inertia of airplanes	M.P. Miller	1-Oct-30	Bifilar	1	1	1	Stated in the report as: “The error has been found to be on the order of 1 percent.”
Tech note 780	Measured moments of inertia of 32 airplanes	W. Gracey	1-Oct-40	Bifilar	2.5	1.3	0.8	Same results as tech note 1629.
Tech note 375	Moments of inertia of several airplanes	Miller, Soule	1-May-31	Bifilar	N/A	N/A	N/A	Only reference to accuracy was that bifilar was 5, 10, and 20 percent more accurate.
Tech note 265	Measurement of the moments of inertia of full scale airplanes	M.W. Green	1-Sep-27	Bifilar	N/A	N/A	N/A	No mention of specific accuracy information.
SAWE Paper No. 2461, Cat. No. 6	A new method for RBP estimation – the dynamic inertia method	M.C. Witter	24-May-99	DIMM	17.69	2.3	0.62	

References

1. Maine, Richard E., and Kenneth W. Iliff, "Application of Parameter Estimation to Aircraft Stability and Control–The Output-Error Approach," NASA RP-1168, 1986.

2. Miller, Marvel P., and Hartley A. Soulé, "Moments of Inertia of Several Airplanes," NACA Technical Note No. 375, May 1931.

3. Turner, Howard L., "Measurement of the Moments of Inertia of an Airplane by a Simplified Method," NACA Technical Note No. 2201, October 1950.

4. Mastinu, G., M. Gobbi, and G. Previati, "A New Test Rig for the Determination of the Inertia Tensor of a Rigid Body," *62nd Annual Conference of Society of Allied Weight Engineers*, Paper No. 3315, May 17, 2003.

5. Witter, M. C., D. L. Brown, and M. Dillion, "A New Method for RBP Estimation–The Dynamic Inertia Method," *58th Annual Conference of Society of Allied Weight Engineers*, Paper No. 2461, May 24, 1999.

6. *Weight Engineer's Handbook*, Society of Allied Weight Engineers, Inc., Los Angeles, May 2008.

7. Berg, Christoph, *The Fundamentals of Weighing Technology: Terms, Methods of Measurement, Errors in Weighing*, Sartorius, 1st ed., 1996.

8. *A Code of Practice for the Calibration of Industrial Process Weighing Systems*, The Institute of Measurement and Control, London, 2003.

9. Marvin, Ron, "Derivation of Formula to Measure Height of Center of Gravity Above a Level Plane," April 2008.

10. Cutright, Amanda, and Brendan Shaughnessy, "New Mass Properties Engineers' Aerospace Ballasting Challenge Facilitated by the SAWE Community," *69th Annual Conference of Society of Allied Weight Engineers*, Paper No. 3497, May 2010.

11. Wolowicz, Chester H., and Roxanah B. Yancy, "Experimental Determination of Airplane Mass and Inertial Characteristics," NASA TR R-433, 1974.